INSTITUTE OF PHYSICS PUBLISHING PLASMA PHYSICS AND CONTROLLED FUSION

Plasma Phys. Control. Fusion **46** (2004) B187–B200 PII: S0741-3335(04)86087-1

The role of energetic particles in fusion plasmas

S D Pinches[1], H L Berk[2], D N Borba[3], B N Breizman[2], S Briguglio[8], A Fasoli[4], G Fogaccia[8], M P Gryaznevich[5], V Kiptily[5], M J Mantsinen[6], S E Sharapov[5], D Testa[4], R G L Vann[7], G Vlad[8], F Zonca[8] and JET-EFDA Contributors[9]

[1] Max-Planck Institut für Plasmaphysik, EURATOM-Assoziation, Boltzmannstraße 2, D-85748 Garching, Germany
[2] Institute for Fusion Studies, University of Texas at Austin, Austin, TX, 78712, USA
[3] Centro de Fusão Nuclear, Associação EURATOM/IST, Instituto Superior Técnico, Av Rovisco Pais, 1049-001 Lisboa, Portugal
[4] CRPP, EPFL, CH 1015 Lausanne, Switzerland
[5] EURATOM/UKAEA Fusion Association, Culham Science Centre, OX14 3DB, UK
[6] Helsinki University of Technology, Association Euratom-Tekes, Finland
[7] Department of Physics, University of Warwick, Coventry, CV4 7AL, UK
[8] Associazione EURATOM-ENEA sulla Fusione, Via E Fermi 45, CP 65-00044 Frascati (Rome), Italy

E-mail: Simon.Pinches@ipp.mpg.de

Received 2 July 2004
Published 17 November 2004
Online at stacks.iop.org/PPCF/46/B187
doi:10.1088/0741-3335/46/12B/017

Abstract

In the burning fusion plasmas of next step devices such as ITER (2001 *ITER-FEAT Outline Design Report* IAEA/ITER EDA/DS/18 (Vienna: IAEA) p 21), the majority of the heating of the fusing fuel will come from the plasma self-heating by fusion born α-particles. Recent advances in theoretical understanding, together with the development of new diagnostic techniques, make this a timely opportunity to survey the role of energetic particles in fusion plasmas and how it projects to future burning plasma devices.

(Some figures in this article are in colour only in the electronic version)

1. Introduction and overview

The sustainment of controlled nuclear fusion requires that the fast charged fusion products produced are confined for a sufficient length of time so as to heat the fuel ions enabling them to fuse and thus achieve a self-sustained burn. Additionally, it is required that they do not adversely affect the stability of the plasma leading to a quench of the fusion process. The role

[9] See annexe 1 of Paméla J *et al* 2002 *Overview of Recent JET Results OV-1/1.4: Proc. 19th Int. Conf. on Fusion Energy 2002 (Lyon 2002)* (Vienna: IAEA).

played by fast particles in reactor-grade plasmas is, therefore, an important one and one which requires careful investigation.

In burning plasma experiments the fusion born α-particles will significantly contribute to the total plasma pressure. The principal concern is that the α-particle population may induce instabilities that cause radial α-particle loss as can happen from the excitation of the toroidal Alfvén eigenmode (TAE). This is an instability that taps the universal instability drive to cause radial displacements of the α-particles. Typically, the universal instability drive is considered a low frequency mechanism that causes the destabilization of drift waves (variants of which are responsible for the anomalous diffusion of the background plasma). However, as the α-particle energy is $\sim$200 times the background plasma energy and the drift frequency of a species is proportional to its energy, this mechanism can cause the destabilization of relatively high frequency waves. In particular, it can cause the destabilization of TAE modes. Indeed, α-particles in tokamak plasmas typically have speeds that are somewhat greater than the Alfvén velocity, and thus the resonant coupling of α-particles to Alfvén waves is quite well matched in future burning plasma experiments.

A fusion reactor can only tolerate fast particle losses of a few per cent primarily due to the first wall damage that they would cause. It is, therefore, important to assess the mechanisms which can lead to the loss of fast ion confinement. These arise principally from two main sources: imperfections in the confining magnetic field structure created by the external coils and self-generated 'imperfections' arising from plasma instabilities. Thus, it is necessary to carefully design magnetic field coils to prevent particle orbit loss in the steady equilibrium fields. In addition, it is essential that any burning plasma experiment has a window of operation where either the TAE modes are stable, or if unstable, the effect of instability leads only to a mild rearrangement of the α-particle distribution, rather than direct loss of α-particles to the surrounding walls. A mild redistribution of the α-particles still allows for the self-heating of the plasma by α-particles. However, direct loss of energetic α-particles attenuates the self-heating in addition to causing wall damage. If a 'sweet spot' with significant self-heating and α-particle production is established, then optimization experiments can be performed to determine the range of plasma parameters that are compatible with ignited operation.

In this tutorial overview a description of energetic particle sources and properties is presented. The area of fast particle driven instabilities is described, in particular the Alfvénic instabilities that occur in toroidal magnetic confinement devices and the impact they have upon energetic particles. Starting from a linear stability analysis the theories are extended into nonlinear regimes, capturing events such as frequency sweeping that arise in response to the redistribution of the energetic particles.

2. Sources of fast ions and fast ion heating

The most promising route to controlled thermonuclear fusion is that based upon fusing the nuclei of hydrogen isotopes, deuterium and tritium:

$$ {}_1\mathrm{D}^2 + {}_1\mathrm{T}^3 \rightarrow {}_2\mathrm{He}^4\ (3.5\,\mathrm{MeV}) + {}_0\mathrm{n}^1\ (14.1\,\mathrm{MeV}). $$

This reaction releases 17.6 MeV of energy, with approximately 20% of the energy released as the kinetic energy of an α-particle (helium nuclei). The fast α-particles created in the D–T reaction are centrally peaked and nearly isotropic in velocity space. They have a well-defined birth energy and they relax due to small angle binary Coulomb collisions with the background plasma from which the characteristic shape of the distribution can be calculated [2]. Above a certain critical fast ion energy, E_{crit}, the power flows primarily to the electrons rather

than to the ions. This critical energy, where the bulk ion friction balances the electron friction, and the power transfer to the electrons is equal to that going to the ions, is given by

$$E_{\rm crit} = 14.8 A_{\rm f} T_{\rm e} \left(\frac{\sum_i n_i (Z_i^2/A_i) \ln \Lambda_i}{n_{\rm e} \ln \Lambda_{\rm e}} \right)^{2/3},$$

where $A_{\rm f}$ and A_i are the atomic masses of the fast and thermal ions, respectively, $T_{\rm e}$ is the electron temperature, n_i and $n_{\rm e}$ are the ion and electron densities and Z_i is the atomic number of the thermal ions. Λ_i and $\Lambda_{\rm e}$ represent the ratio between the Debye length and the distance of closest approach in classical Coulomb scattering theory. For a 50 : 50 D : T mixture in JET, the critical energy below which collisions with ions start to dominate is $E^{\alpha}_{\rm crit} \approx 33 T_{\rm e}$. Thus, for a burning plasma with $T_{\rm e} \sim 20$ keV, $E^{\alpha}_{\rm crit} \approx 650$ keV and most of the α-particle energy (3.5 MeV) directly heats the electrons. Typically, the D–T fuel will have a temperature 1–2 keV below the electron temperature with the precise value determined by the overall ion energy confinement time in the burning plasma.

For the case of D–T reactants sharing a common temperature, $T_{\rm i}$, α-particles are produced at a birth energy of $E_0 = 3.5$ MeV with an energy distribution of the form, $S(E) = S_0 \exp[-(E - E_0)^2/\Delta E^2] \approx S_0 \delta(E - E_0)$ where $S_0 = \langle n_{\rm D} n_{\rm T} \sigma_{\rm DT} v \rangle$. The energy distribution from the solution of the collisional equation is then the so-called slowing down distribution that arises due to drag from the thermal particles acting on the α-particles [3],

$$f(E) = \frac{C}{E^{3/2} + E_{\rm crit}^{3/2}} \, {\rm Erfc}\left[\frac{E - E_0}{\Delta E} \right] \approx \frac{C}{E^{3/2} + E_{\rm crit}^{3/2}} H(E_0 - E), \tag{1}$$

where ${\rm Erfc}(x)$ is the complementary error function and $H(x)$ is the Heaviside function. C is an appropriate constant proportional to S_0 and the slowing down time for α-particles, $\tau_{\rm s} \approx 10^6 T_{\rm e}^{3/2}({\rm keV})/n_{\rm e}({\rm m}^3)$.

There are other sources of energetic particles that are also expected to be present in future reactors. These sources include fast ions produced by auxiliary heating systems such as neutral beam injection (NBI) and radio-frequency (RF) heating. The fast ions created by NBI have a 'birth' energy defined by the accelerating electric potential of the injection system typically in the 50–100 keV range in present-day experiments and comparable to the MeV range in burning plasma experiments such as ITER [1]. Due to the geometry of the NBI source their angular distribution is anisotropic and their spatial distribution depends upon the injection energy and plasma density along the beam line.

Energetic particles created from the heating of a minority ion species by RF waves in the ion cyclotron frequency range (ICRF) do not have a sharp high energy cut-off and possess a highly anisotropic velocity distribution function associated with the way the RF waves couple power to the particles' motion perpendicular to the magnetic field. ICRH heated minority ions can reach energies in the MeV range making it an important heating source to study the effects of highly energetic particles [4]. In the steady state, the balance of ICRF heating and electron drag determines their energy distribution [5].

The classical behaviour of α-particle heating was verified on TFTR [6] and JET [7–9]. A scan of the D–T mixture was used on JET to unambiguously measure an increase in the central electron temperature of 1.3 ± 0.23 keV due to 1.3 MW of α-heating [7]. With a plasma energy confinement time of 1.2 s, the α-heating produced an increase in the plasma energy content of more than 1 in 9 MJ. This indicates that in these experiments α-heating was as effective as hydrogen minority ICRH. These experimental results thus show that for the case of moderate α-particle heating there are no unpleasant surprises. Indeed, the JET D–T plasmas support the basic theoretical understanding. In later sections we consider the transfer of α-particle energy into less constructive channels, namely into collective instabilities that could potentially lead to

fast particle redistribution or loss. Such effects may occur with increased heating by α-particles as may occur in a burning plasma.

3. Fast particle confinement

One of the most basic requirements for confining fast particles in a magnetic confinement system is that their radial excursion as they move through the plasma must be much smaller than the radial extent of the plasma. For a given particle energy and a given confining field strength, this favours larger devices. For trapped particles in a tokamak plasma, i.e. those particles with typically the largest radial deviation, this radial excursion is given by $\Delta r = m v_\parallel / e B_\mathrm{p}$, where m and e are the fast particle mass and charge, respectively, $v_\parallel$ is the particle's velocity component parallel to the magnetic field and B_p is the poloidal magnetic field strength determined by the toroidal plasma current, I_p (see e.g. [10]). Using Ampère's law to relate B_p to I_p, the requirement that $\Delta r < a$ can be expressed as a restriction on the plasma current, namely, $I_\mathrm{p} > 2\pi m v_\parallel / \mu_0 e$. Thus, the threshold to confine a 3.5 MeV α-particle requires $I_\mathrm{p} > 1.5$ MA, as confirmed by recent trace tritium experiments on JET [8, 9].

One of the main predicted single particle loss mechanisms for α-particles in a future reactor is toroidal magnetic field (TF) ripple (owing to the non-axisymmetric variation of the field due to the finite number of toroidal field coils) induced stochastic diffusion (see [11] and references therein). The orbits of ripple trapped banana particles are not closed and their turning points experience a small, but finite vertical displacement after each bounce. When the vertical excursions of the banana-tips exceed a certain threshold, stochasticity occurs, leading to a diffusion-like phenomenon [12]. The resulting diffusion coefficient depends both on the ripple magnitude, $\delta \equiv (B_\mathrm{max} - B_\mathrm{min})/(B_\mathrm{max} + B_\mathrm{min})$ and the particle energy. When the ripple is important, particles are lost within a few hundred bounces; a time much shorter than their slowing down time.

Controlled experiments were performed in JET in the early 1990s to investigate the influence of the TF ripple on the confinement of fast ions in the range from $\sim$100 keV to $\sim$3 MeV [13]. Using only 16 out of the 32 TF coils available at JET resulted in an increase of the ripple, which had a detrimental effect on the plasma behaviour. Comparing 16 coil discharges with 32 coil reference discharges led to a reduction in the total stored plasma energy of NBI heated L-mode plasmas by $\sim$30% and a reduction of the ion heating. Thus, these experiments demonstrated how the confinement of energetic particles is degraded in the presence of a toroidal field ripple.

4. Instability mechanisms and linear Alfvén eigenmodes

It is well known that confined plasmas of species j have a flow, generally called the diamagnetic drift flow,

$$\boldsymbol{v}_{*j} \approx \frac{1}{e_j B_j} \frac{\boldsymbol{b} \times \nabla (n_j E_j)}{n_j},$$

where n_j is the density of species j, q_j its charge and E_j its mean energy. Further, if $0 < \omega < \langle \boldsymbol{k} \cdot \boldsymbol{v}_{*i} \rangle$ (where $\boldsymbol{k}$ is the mode number and $\langle \cdots \rangle$ denotes spatial averaging) particle resonance gives rise to an inverse dissipative contribution that can destabilize a wave (the so-called universal instability drive). In thermal plasmas, this mechanism is known to contribute to anomalous diffusion where it acts at relatively low frequencies. However, as $\omega_\alpha \propto \langle E_\alpha \rangle \sim 200T$ (keV), energetic particles can destabilize waves at relatively high frequencies, in particular shear Alfvén waves. In ideal MHD the shear Alfvén dispersion

relation is $\omega^2 = k_\parallel^2 v_A^2$, where $v_A = \sqrt{B_0^2/\mu_0\rho_0}$ is the Alfvén speed. Shear Alfvén waves represent a balance between plasma inertia and field line tension and are analogous to waves on a taut string.

In inhomogeneous plasmas, such as those found in all magnetically confined fusion grade devices where the density, n, and thus the Alfvén speed, depend upon the minor radius, r, the shear Alfvén dispersion relation becomes $\omega^2 = k_\parallel^2(r) v_A^2(r)$. It is clear that no wave packet of finite radial extent can persist for long since each radial 'slice' along the wave packet moves with a different velocity in a different direction. This effect, known as phase mixing [14] effectively leads to the damping of any initial Alfvén waves in an inhomogeneous plasma. It was mainly for this reason that Alfvén instabilities driven by energetic particles were initially not considered a threat to future tokamak reactors. This view changed with the discovery of weakly damped global Alfvén eigenmodes (GAEs) [15,16] and weakly damped TAEs [17,18]. The former are often observed in stellarators [19] whilst the latter are particularly relevant for tokamak burning plasmas [20].

5. Toroidal Alfvén eigenmodes

In a torus it is natural to represent perturbations of the plasma by Fourier decomposition into poloidal, m, and toroidal, n, harmonics, $\xi(r, \theta, \phi) = \sum_{m,n} \xi_{m,n}(r) \exp[\mathrm{i}(n\phi - m\theta - \omega t)]$. Since the equilibrium magnetic field, $B \approx B_0 R_0/R \approx B_0(1 - r/R_0 \cos\theta)$, is a function of θ, a coupling arises between the neighbouring poloidal harmonics and, to lowest order in the inverse aspect ratio, $\varepsilon = r/R_0 \ll 1$, each poloidal harmonic, m, couples to its nearest neighbouring sidebands, $m \pm 1$. The parallel wave number is approximately given by $k_{\parallel m} = 1/R(n - m/q(r))$, where q is the so-called safety factor (the inverse of the field helicity, ι) and can be approximated as $q(r) = r B_t/R B_p$ where r is the minor radius, R the major radius and B_p and B_t are the poloidal and toroidal magnetic field components, respectively. In this case, the system is described by a set of coupled differential equations for the radial plasma displacement [18].

There is, however, a special degeneracy in a cylinder where the various branches of the Alfvén continuum cross each other (in the case of figure 1 only two branches are shown). This occurs when $\omega = -k_{\parallel m+1}(r) v_A(r) = +k_{\parallel m}(r) v_A(r)$, which is satisfied where $q(r) = (2m + 1)/2n$. Near such points in a torus, toroidal coupling resolves the degeneracy by developing a band gap in frequency where phase mixing does not occur.

Within the frequency gap, new eigenmode solutions have been found to exist known as TAEs. Since these modes lie within this frequency gap in the Alfvén continuum they do not experience continuum damping and are, therefore, damped by weaker dissipative processes. These modes are spatially localized around the extremum of ω^2 and typically consist of the two main poloidal harmonics that are associated with the gap. A typical example is shown in figure 1(*b*). Besides TAE, additional coupling mechanisms due to the shaping of the plasma's poloidal cross-section allow other gaps to appear in the Alfvén frequency continuum, which support other eigenmodes such as the elliptical Alfvén eigenmode (EAE) and the non-circular Alfvén eigenmode (NAE).

6. Alfvén cascades

A very interesting example of Alfvén instabilities, differing from TAEs, is the Alfvén cascades (ACs) [21–23] observed for the first time on JT-60U [24], and routinely detected in JET optimized shear experiments as the non-monotonic safety factor profile evolves. A series of

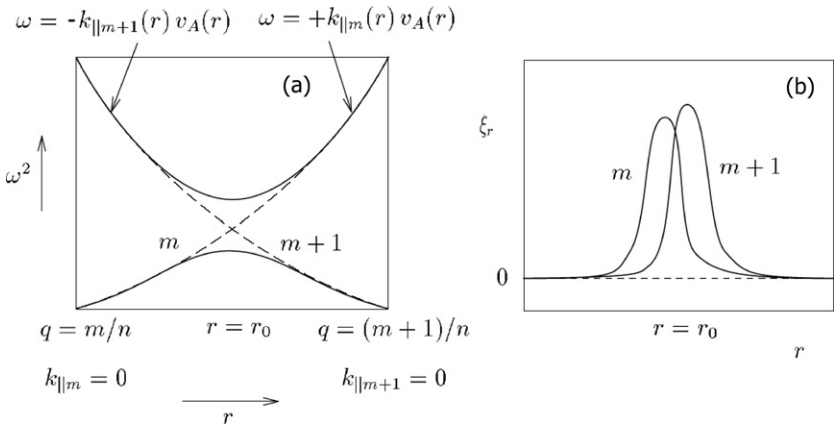

Figure 1. (*a*) Alfvén frequency continuum in a torus showing coupled poloidal harmonics and (*b*) the corresponding TAE eigenfunction.

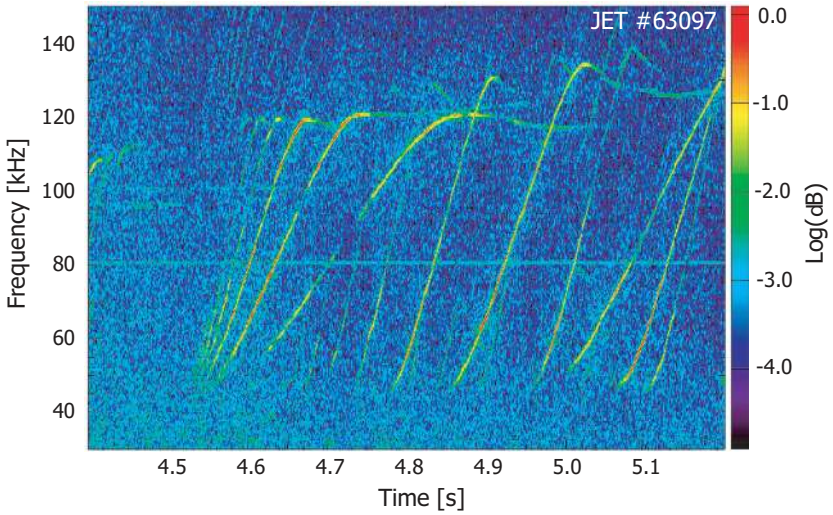

Figure 2. Spectrogram made from edge magnetic measurements in JET #63097 showing upward sweeping ACs and their transition into TAEs.

upward frequency sweeping Alfvén modes are observed as seen in figure 2, driven by the ICRH heating [21]. The AC consists of many modes with different toroidal mode numbers and different frequencies. The toroidal mode numbers vary from values as low as $n = 1$ to values as high as $n = 16$. Their frequency typically starts from around 20–60 kHz, i.e. well below the TAE frequency, and sweeps up to the frequency of the TAE-gap. The rate of increase of the AC frequency is found to be proportional to the toroidal mode number, n, and they occur when the Alfvén continuum has a *maximum* at $q_{\min}$ [21–23].

The theoretical interpretation of ACs was given in [22,25,26] in terms of an Alfvén mode localized at the point where $q(r)$ has a minimum, $q_{\min}$ (point of zero magnetic shear), with a dispersion relation,

$$\omega(t) = \left| \frac{m}{q_{\min}(t)} - n \right| \cdot \frac{v_{\mathrm{A}}(t)}{R_0} + \Delta\omega. \tag{2}$$

Here, $q_{\min}(t)$ and $v_A(t)$ vary in time in accordance with the experiment and $\Delta\omega$ is a small offset frequency that depends upon the fast ion pressure β_{hot}, the second derivative d^2q/dr^2 and $(r/R)^2$ at $q_{\min}$. Due to the finite value of $\Delta\omega$ the AC is not subject to significant continuum damping. Note also from equation (2) that $d\omega(t)/dt = mv_A/R_0(d/dt)q_{\min}^{-1}(t)$ and faster frequency sweeping arises for higher $m \approx nq_{\min}(t)$, in accordance with the experimental results. Thus, for example, the $n = 1$ mode occurs when $q_{\min}$ passes integer values 1, 2, 3, ...; the $n = 2$ mode occurs when $q_{\min}$ passes integer and half-integer values 1, $\frac{3}{2}$, 2, $\frac{5}{2}$, ...; and the $n = 3$ mode occurs when $q_{\min}$ passes 1, 1.33, 1.67, 2, 2.33, ... etc. It was found on JET [21] that the clustering pattern of cascades with different mode numbers allows the evolution of $q_{\min}(t)$ to be accurately determined, greatly facilitating the development of scenarios containing transport barriers [27, 28].

7. Stable Alfvén eigenmodes

When the fast particle drive is insufficient to overcome the various damping processes present, the Alfvén eigenmodes (AEs) are stable and cannot be directly observed. However, driving low amplitude ($\delta B/B \sim 10^{-6}$) waves in the plasma using an external antenna and measuring the plasma response allows the frequency and damping rate of stable AEs to be measured [29, 30]. Using this technique it has been possible to characterize the effects of plasma shape [31], ρ_* [32] and β [33] on the AE damping rates in JET [34].

8. Nonlinear Alfvén eigenmode dynamics

Linear theory gives an indication of whether α-particles (perhaps together with neutral beams) will drive instabilities in a burning plasma. Studies [35] indicate that Alfvénic driven instabilities are likely to arise over pertinent regimes, especially as the plasma temperature goes beyond 20 keV. However, the question remains as to whether α-particles will be lost, or simply redistributed within the plasma during Alfvénic instability. In some experiments with relatively high neutral beam power [36–38], energetic particle populations have been observed to be affected by the presence of TAE excitation. In other experiments [39] TAE activity is observed without significant energetic particle losses. It is also clear that larger machines, such as ITER, can allow for considerable α-particle redistribution without loss. In general, nonlinear theory is not as yet sufficiently well developed to reliably predict the α-particle losses due to instability. A full theory will also have to account for the energetic particle re-distribution due to the synergistic effect of Alfvénic instability with other superimposed perturbations, ranging from transient sawtooth (or giant sawtooth) oscillations to steady-state imperfections in the magnetic fields that give rise to ripple loss of trapped particles near the plasma edge [40].

The α-particle Alfvénic wave problem has allowed a very basic approach in the study of the development of diffusive processes of particles acted on by waves and the feedback of the currents generated by such a perturbation to the waves. We consider the case where the waves are perturbative and there are only a few modes present so that these modes can be viewed as being discrete. Most of the energetic particles then respond adiabatically to the waves and their distribution function is barely even distorted. Only a minority of the energetic particles will then resonate with the waves. The result of interaction can be a relaxation of the distribution in the resonant region so as to quench the universal instability drive by eliminating the local spatial gradient in the distribution function. This has been shown to be the case when the linear instability drive is substantially larger than the background dissipation. If the energetic particles can be considered as collisionless, saturation occurs when the trapping

frequency of the energetic particles in the wave (proportional to $\delta B^{1/2}$) is equal to the linear growth rate. One can also show that the particle displacements are proportional to $\delta B^{1/2}$ and that this displacement can be viewed as the intrinsic width of a resonance. The appropriate proportionality coefficients are readily calculated and, in principle, assessments can be made about whether modes overlap. The effect of overlap has been studied in [41] and it is shown that mode overlap can lead to a rapid transition from low level benign oscillations, to much higher level oscillations accompanied by rapid energetic particle diffusion within a large region of the plasma.

A deep insight into the nature of the evolution of mode response arose [42] as a result of viewing the evolution of kinetic instabilities near the marginal stability point. This is where the instability drive (e.g. from the universal instability drive associated with energetic particles acting on Alfvén-like waves) is nearly balanced by background dissipation processes. In this case, a very important parameter in nonlinear theory is $\nu \equiv \nu_{\rm eff}/\gamma$, where $\nu_{\rm eff}$ is the effective collision frequency, while the linear growth rate is $\gamma = \gamma_{\rm L} - \gamma_{\rm d}$ with $\gamma_{\rm L}$ the growth rate from energetic particles neglecting dissipation, and $\gamma_{\rm d}$ the damping rate of the mode due to background dissipation neglecting the energetic particle drive. A cubic nonlinear temporally non-local equation was derived [42] that depends on the single control parameter ν. In essence, the parameter ν describes the competition between the field of the wave that is trying to flatten the resonant particle distribution function and the relaxation processes that are continually trying to restore it.

It was found that the effects of collisions on resonant particles are more important in the nonlinear regime than in the linear regime, which is quite insensitive to such details. Numerical solutions [42] of this equation to determine the evolution of the mode amplitude have shown that at high collision frequencies, $\nu > 4.4$, a linear growth phase is followed by a saturated level ([42], see figure 2). At lower collisionalities, $\nu < 4.4$, the solution starts to pulsate with the oscillations becoming more complex and irregular as the collision frequency is further lowered. These solutions show a well-defined sequence of transitions as ν is decreased from periodic, through multiply periodic, to chaotic behaviour and finally explosive behaviour when the assumptions in the derivation of the theory break down at sufficiently large amplitudes. It is possible to consider the saturated steady-state solution of the system as a fixed point of the system dynamics [42]. The path to chaos then corresponds to a series of pitchfork bifurcations of this initially stable fixed point. This bifurcation picture has been qualitatively reproduced in fully nonlinear particle simulations by Vann *et al* [43–45].

Observations of TAE splitting in JET by Fasoli *et al* [46] have been interpreted in terms of a slight extension of this model (where a second parameter is introduced as a result of finite $\gamma_{\rm L}/\omega$). In figure 3 several linear TAE modes (of different toroidal mode numbers) are simultaneously self-excited soon after the energetic neutral beam heating was applied. The frequencies slowly change in time due to the evolving plasma equilibrium. Initially, there are well-defined single spectral lines but these lines begin to split with increased structure as time evolves. The cubic nonlinear equation with a time evolving ν (primarily due to an increasing population of energetic particles) was used to explain the frequency splitting structure. Figure 3 also shows a comparison of JET data with results that emerge from the solution of the cubic nonlinear equation as the parameter $\nu(t)$ varies. The precision of the matching enabled the determination of the mode growth rates and effective collision frequencies [46].

To investigate what happens beyond the explosive phase a kinetic simulation model was developed [47]. It was found that the wave grows to a level where the trapping frequency of the resonant particles becomes comparable with the linear growth rate. Instead of the wave damping, as might be expected if the source of instability is depleted through the local flattening of the appropriate gradient of the distribution in the resonance region, the wave amplitude remained

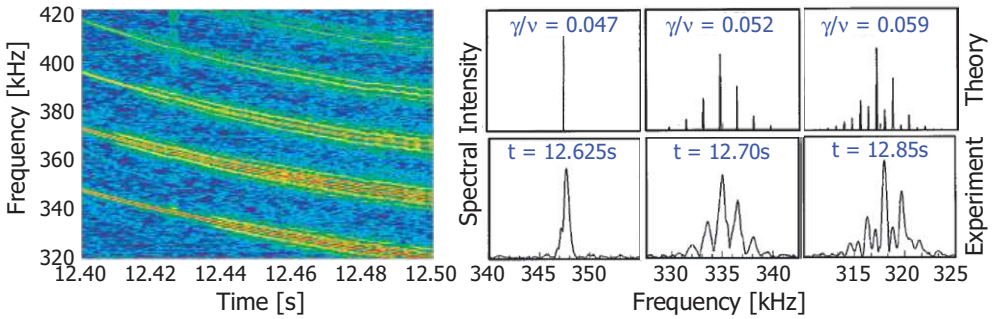

Figure 3. (Left) Spectrogram of edge magnetic activity in JET hot-ion H-mode #40332 showing the appearance of ICRH driven TAE ($P_{\mathrm{ICRH}} \sim 6.5$ MW). (Right) Nonlinear splitting of TAE spectral lines for this case. Note the good agreement between theory and experiment for the asymmetries in the spectral line splitting.

roughly constant for many damping times. It was observed that the wave undergoes significant frequency sweeping and it was realized that it was this frequency sweeping that enables the destabilizing kinetic distribution to match the power that is being absorbed by the background dissipation mechanisms. Indeed, a trapped phase space structure spontaneously forms to give rise to frequency up-shifting and down-shifting nonlinear Bernstein–Greene–Kruskal (BGK) modes. The distribution function in the trapping regions remains at the same value as the equilibrium distribution function at the linear phase velocity even as the phase space structures change their phase velocities. This can be seen in the evolution of the phase-space structures ([47], see figure 3). The qualitative and quantitative description of the mechanisms of enabling a nonlinear frequency shifted trapped particle mode [48] together with the power balance relation is described in [47]. The mechanisms lead to a frequency sweeping prediction and mode amplitude (when $t \ll 1/\nu_{\mathrm{eff}}$) given by $\omega_{\mathrm{b}} \cong 0.5\gamma_{\mathrm{L}}$ and $\delta\omega \cong 0.4(\gamma_{\mathrm{d}}/\gamma_{\mathrm{L}})^{1/2}\ \gamma_{\mathrm{L}}^{3/2} t^{1/2}$. This scaling, together with coefficients, were even found to apply in simulations where multiple resonances (due to a TAE mode) were simultaneously present. Note that the saturated amplitude (measured by $\omega_{\mathrm{b}} \propto A^{1/2}$, where A is the mode amplitude) is simply related to γ_{L}. Hence, if nonlinear phase-space structures of the character being described are self-excited in experiments, it is then possible to estimate the internal perturbed fields spectroscopically by observing the time scale of the frequency sweep. Frequency sweeping data, which are good candidates for the formation of phase space structures by means of the model that is being described here, have been observed in several TAE studies [49–51].

The MAST data shown in figure 4 [50] have been studied in some detail [51] in an effort to ascertain whether the field amplitude inferred from the frequency sweeping theory is consistent with the observed amplitudes measured with Mirnov coils. In applying the theory, the drift-kinetic δf simulation code HAGIS [52, 53] was used to find the relationship between mode amplitude, ω_{b}, and γ_{L}. These relationships were used in HAGIS to verify the consistency of frequency sweeping and mode amplitude predictions. In figure 5 we see that a down-sweeping phase space 'clump' (for a clump, the trapped particle distribution is larger than the immediately surrounding ambient passing particle distribution) was formed. The simulations showed that the frequency sweeping follows the predicted theory for the time scale that was observed and that the mode amplitude closely matches the level predicted by the mode sweeping theory.

The same procedure was used to infer the mode amplitude in the MAST data shown in figure 4. It was found that the mode amplitude inferred from frequency sweeping analysis was about half that inferred from external Mirnov coil measurements. This good correlation shows consistency between the proposed frequency sweeping mechanism and the data.

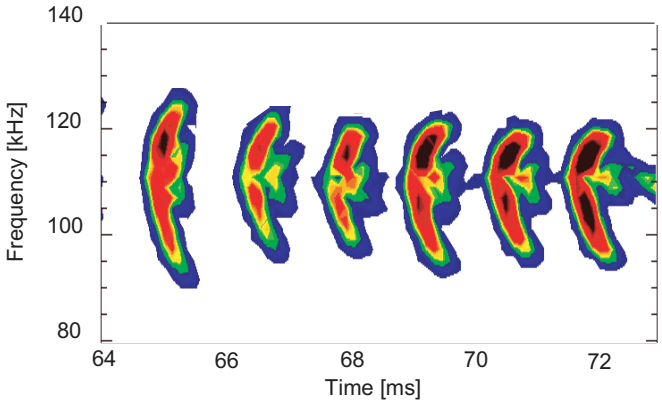

Figure 4. Frequency sweeping AE in MAST #5568.

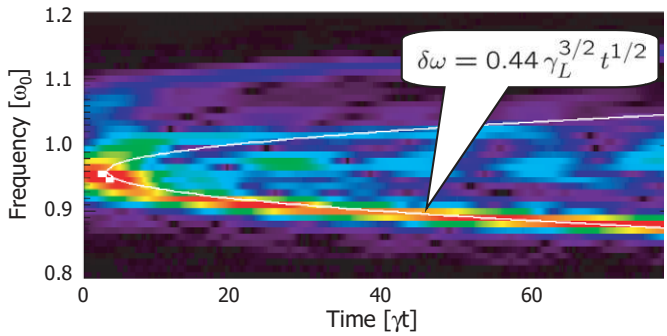

Figure 5. Sliding Fourier spectrum showing frequency evolution of marginally unstable TAE mode in response to kinetic α-particle drive ($\gamma_L/\omega_0 = 0.45\%$) and external damping ($\gamma_d/\omega_0 = 0.4\%$). The over-plotted white line shows the theoretically predicted frequency sweeping rate of $0.4\gamma_L(\gamma_d t)^{1/2}$.

There are modes in tokamaks that sweep in frequency, such as for example, the so-called fishbone mode [54, 55]. In its initial phase, this mode is non-perturbative and does not fit the early stages of the Berk–Breizman model. Nonetheless, in the late stages these modes have well resolved chirping frequency and interesting similarities with the frequency sweeping events described above (see, for example, White–Boozer model [56]).

9. Non-perturbative energetic particle modes

The previous sections describe the interaction of energetic particles with Alfvén waves that can be supported by the background plasma. However, when there is a sufficiently large energetic particle population, these particles can alter the plasma mode characteristics. As a result, new modes of a shear-Alfvénic character (energetic particle modes or EPMs) can arise that do not exist in the absence of these energetic particles (hence the classification as non-perturbative modes). These modes are particularly easy to establish in regions of low magnetic shear. Additionally, as the normalized plasma pressure, $\beta = \langle p \rangle (B^2/2\mu_0)$, is increased, conventional TAE are suppressed but EPMs can still arise. Extensive analysis of this class of modes is presented in [57, 58].

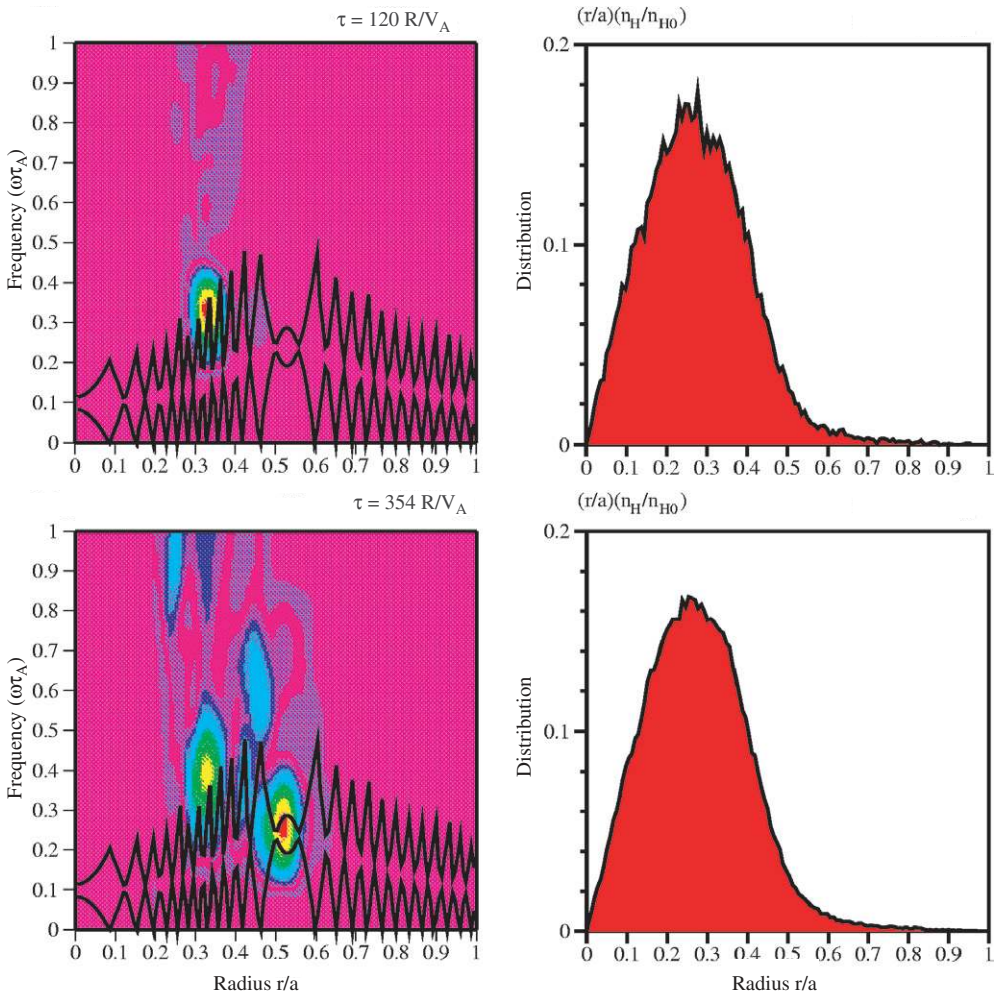

Figure 6. The left frames show a mode intensity contour plot in the $(r/a, \omega\tau_A)$ plane, where $\tau_A = R_0/v_A(0)$, for two times: $t = 120\tau_A$ and $t = 354\tau_A$ with the Alfvén continuum over-plotted. The fast ion surface density, $(r/a)(n_H/n_H(0))$ is shown in the right frames.

In the case of hollow-q profiles and strong ICRH heating, Alfvén modes can be excited at different radial locations: ACs are localized near the q-minimum surface, whereas strong resonant excitation of EPMs [57] should occur where $\alpha_H = -R_0 q^2 \beta'_H$ is maximum. This typically occurs inside the q-minimum surface when the threshold condition for resonant EPM excitation is exceeded [58].

For nominal fast ion distribution values illustrated by JET discharge #49382, i.e. $\beta_H(0) = 0.008$ and $\alpha_{H,max} = 0.55$ at $r/a = 0.2$, nonlinear hybrid MHD-gyrokinetic simulations with the HMGC code [59] shown in figure 6 [58] demonstrate the early resonant excitation of an EPM inside the q-minimum surface, followed by the later formation of a cascade mode at the q-minimum surface. In this case of moderate drive, the EPM and AC have independent nonlinear dynamics and the fast particle transport is weak and diffusive, as can be seen from the right column of figure 6, which is not significantly altered in the nonlinear phase. Experimental

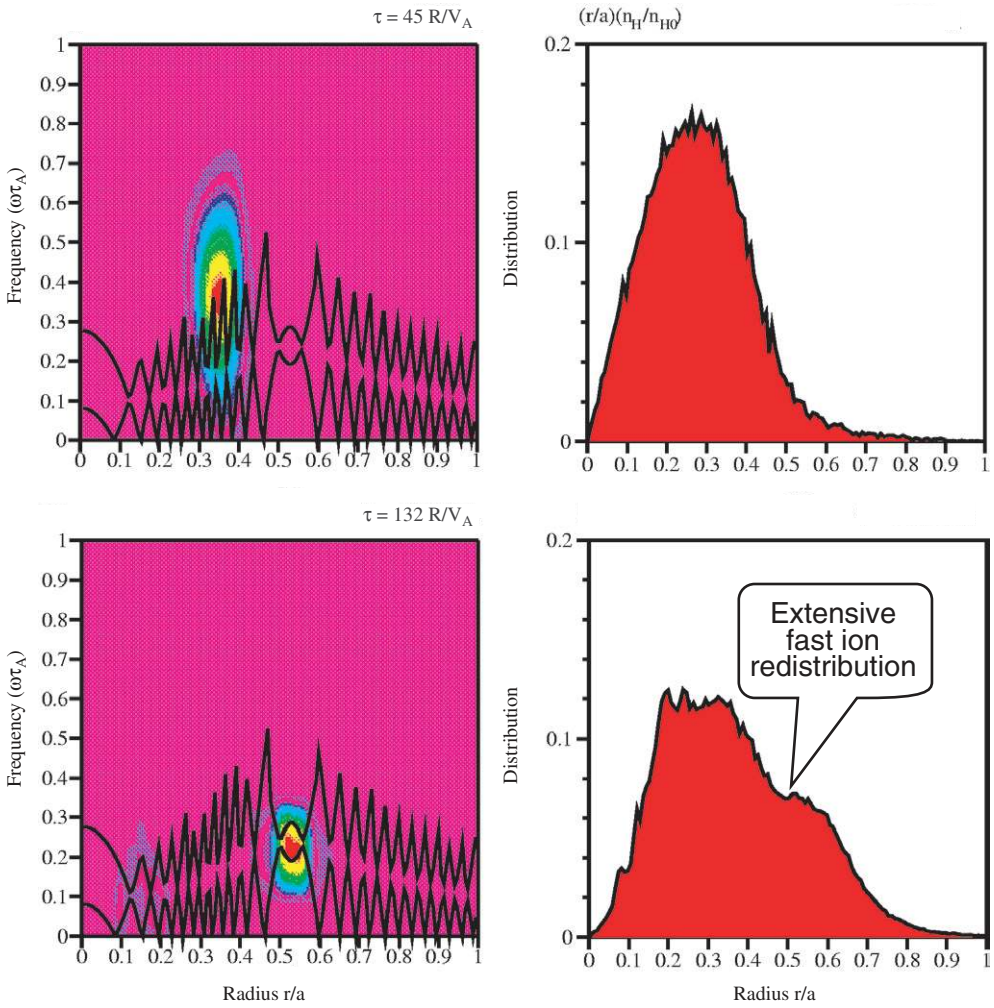

Figure 7. Same as figure 6, at fixed profiles but with $\beta_{H0} = 0.022$. Times shown are $t = 45\tau_A$ and $t = 132\tau_A$. The latter time point corresponds to the fully nonlinear saturated state and shows significant, rapid, radial transport of the fast ions.

profiles are thus expected to be close to those predicted on the basis of power deposition calculations.

For the same profiles, but with $\beta_{H0} = 0.022$, i.e. $\alpha_{H,max} = 1.5$ at $r/a = 0.2$, the nonlinear evolution is shown in figure 7, where the left frames indicate that the core localized EPM is characterized by a rapid nonlinear evolution and an outward radial displacement, accompanied by a downward chirping frequency, which eventually stops when the mode merges into a cascade mode [58]. This process corresponds to a strong convective redistribution of fast ions, as visible in the frames on the right. Experimental profiles in this strong drive case are expected to differ from power deposition predictions.

Note that the time scale for these dynamics is the inverse growth rate, $1/\gamma_L \sim O(100R_0/v_A)$, i.e. much faster than that of the quasi-static equilibrium modifications due to current diffusion and responsible for the experimentally observed frequency dynamics of

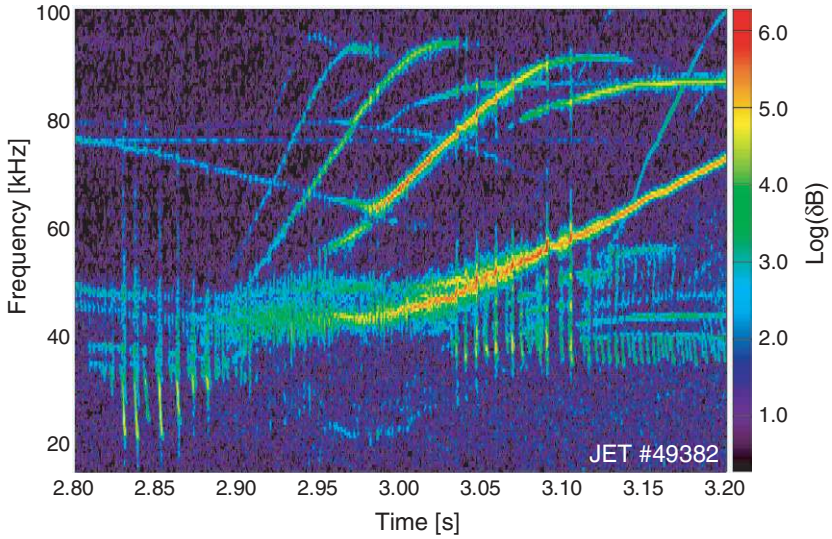

Figure 8. JET #49382 showing slow upward sweeping ACs and repeated rapid down-sweeping modes.

the ACs. The EPM induced fast frequency chirping is always downward, being associated with fast ion outward radial transport. This could be the explanation of the fast frequency sweeping shown in figure 8 superimposed on the slower frequency dynamics of the AC.

10. Summary and outlook

The role played by energetic particles is central to the success of future burning plasma experiments such as ITER. From the experiments carried out to date [6, 7], the bulk plasma heating is as theoretically predicted from the underlying physical processes and in this aspect, there appears to be no cause for concern. Collective instabilities driven by energetic particles (in particular TAE) have been shown to lead to significant losses of fast particles [36–38], reassuringly, however, at higher current in JET [39], this was not found to be the case. The theoretical understanding of the principal Alfvénic instabilities is progressing well and is now able to yield valuable diagnostic information (see, for example, [26, 49]).

References

[1] *ITER-FEAT Outline Design Report* 2001 IAEA/ITER EDA/DS/18 (Vienna: IAEA) p 21
[2] Heidbrink W W and Sadler G 1994 *Nucl. Fusion* **34** 535
[3] Gaffey J D 1976 *J. Plasma Phys.* **16** 149
[4] Mantsinen M J *et al* 2003 *Plasma Phys. Control. Fusion* **45** A445
[5] Stix T H 1979 *Nucl. Fusion* **15** 737
[6] Taylor G *et al* 1996 *Phys. Rev. Lett.* **76** 2722
[7] Thomas P R *et al* 1998 *Phys. Rev. Lett.* **80** 5548
[8] Kiptily V *et al* 2004 *Phys. Rev. Lett.* submitted
[9] Kiptily V *et al* 2004 *31st EPS Conf. on Plasma Physics (London)* O1-06
[10] Wesson J 2004 *Tokamaks* 3rd edn (Oxford: Oxford University Press)
[11] White R B *et al* 1989 *Proc. 12th Int. Conf. on Plasma Phys. Control. Nucl. Fusion (Nice, 12–19 October 1988)* IAEA-CN-SOD-11-4 *Nucl. Fusion* **2** (Suppl.) 111
[12] Goldston R G, White R B and Boozer A H 1981 *Phys. Rev. Lett.* **47** 647–8

[13] Sadler G *et al* 1992 *Plasma Phys. Control. Fusion* **34** 1971–6
[14] Tataronis J and Grossman W 1973 *Z. Phys.* **261** 203
[15] Appert K, Gruber R, Troyon F and Vaclavik J 1982 *Plasma Phys.* **24** 9
[16] Ross D W, Chen G L and Mahajan S M 1982 *Phys. Fluids* **25** 4
[17] Cheng C Z, Liu Chen and Chance M S 1985 *Ann. Phys.* **161** 21
[18] Cheng C Z and Chance M S 1986 *Phys. Fluids* **29** 3695
[19] Weller A *et al* 1994 *Phys. Rev. Lett.* **72** 1220–3
[20] Sharapov S E *et al* 2000 *Nucl. Fusion* **40** 7
[21] Sharapov S E *et al* 2001 *Phys. Lett.* A **289** 127
[22] Berk H L *et al* 2001 *Phys. Rev. Lett.* **87** 185002
[23] Sharapov S E *et al* 2002 *Phys. Plasmas* **9** 2027
[24] Kimura H *et al* 1998 *Nucl. Fusion* **38** 1303
[25] Breizman B N *et al* 2003 *Phys. Plasmas* **10** 3649
[26] Borba D N *et al* 2002 *Nucl. Fusion* **42** 1029
[27] Joffrin E *et al* 2003 *Nucl. Fusion* **43** 1167
[28] Pinches S D *et al* 2003 *30th EPS Conf. on Control. Fusion and Plasma Phys. (St Petersburg) (Europhysics Conference Abstacts)* vol 27A P1.93
[29] Fasoli A *et al* 1995 *Phys. Rev. Lett.* **75** 645
[30] Fasoli A *et al* 2000 *Phys. Plasmas* **7** 1816
[31] Testa D and Fasoli A 2001 *Nucl. Fusion* **41** 809
[32] Testa D, Fu G Y, Jaun A, Fasoli A and Sauter O 2003 *Nucl. Fusion* **43** 479
[33] Testa D, Fasoli A and Jaun A 2003 *Nucl. Fusion* **43** 724
[34] Fasoli A *et al* 2000 EXP2/04 *18th IAEA Fusion Energy Conf. (Sorrento)*
[35] Gorelenkov N N *et al* 2003 *Nucl. Fusion* **43** 594–605
[36] Heidbrink W W *et al* 1991 *Nucl. Fusion* **31** 1635
[37] Wong K L *et al* 1991 *Phys. Rev. Lett.* **66** 1874
[38] Duong H H *et al* 1993 *Nucl. Fusion* **33** 749
[39] Borba D N *et al* 2000 *Nucl. Fusion* **40** 775
[40] White R B *et al* 1995 *Phys. Plasmas* **2** 2871
[41] Berk H L, Breizman B N and Pekker M S 1995 *Nucl. Fusion* **35** 1713
[42] Berk H L, Breizman B N and Pekker M S 1996 *Phys. Rev. Lett.* **76** 8
[43] Vann R G L *et al* 2003 *Phys. Plasmas* **10** 623
[44] Vann R G L *et al* 2004 *Proc. 31st EPS Conf. on Plasma Phys.* P1-113
[45] Vann R G L, Dendy R O and Gryaznavich M P 2004 *Phys. Plasmas* submitted
[46] Fasoli A *et al* 1998 *Phys. Rev. Lett.* **81** 25
[47] Berk H L, Breizman B N and Petviashvili N V 1997 *Phys. Lett.* A **234** 213
Berk H L, Breizman B N and Petviashvili N V 1998 *Phys. Lett.* A **238** 408 (erratum)
[48] Kruer W L, Dawson J M and Sudan R N 1969 *Phys. Rev. Lett.* **23** 838
[49] Kramer G J *et al* 2000 *Nucl. Fusion* **40** 1383
[50] Gryaznevich M P and Sharapov S E 2004 *Plasma Phys. Control. Fusion* **46** S15
[51] Pinches S D *et al* 2004 *Plasma Phys. Control. Fusion* **46** S47
[52] Pinches S D 1996 *PhD Thesis* The University of Nottingham
[53] Pinches S D *et al* 1998 *Comput. Phys. Commun.* **111** 131
[54] Chen L, White R B and Rosenbluth M N 1984 *Phys. Rev. Lett.* **52** 1122
[55] Coppi B and Porcelli F 1986 *Phys. Rev. Lett.* **57** 2272
[56] White R B *et al* 1983 *Phys. Fluids* **26** 2958
[57] Chen L 1984 *Phys. Plasmas* **1** 1519
[58] Zonca F *et al* 2002 *Phys. Plasmas* **9** 4939
[59] Briguglio S, Vlad G, Zonca F and Kar C 1995 *Phys. Plasmas* **2** 3711